

Main S&T results/foregrounds

WP2: Fabrication and Structural Optimisation of Silicon Nanocrystals in Selected Host Materials

WP2 was focused on the fabrication and structural optimization of Silicon nanocrystals in selected host materials, i.e. either SiO_2 or SiC or Si_3N_4 . The reason for testing the different materials is related to the respective significant differences in optical and electronic properties of the respective matrix materials. Where the SiO_2 material has advantages for quantum confinement the SiC or Si_3N_4 material has better transport properties. Thus, compromises are needed in case of using the quantum confined Si nanocrystals for applications such as solar cells. The WP2 was divided into 3 milestones. MS1 (M12) was focusing on the fabrication of Si quantum dots with optimized density, band gap and a high absorption. MS2 (M24) was related to the development of doped multilayers with optimized structural and electrical properties and MS3 (M30) to the optimized growth process (i.e. thermal budget) adapted to back and top cell configurations.

For the sample fabrication, plasma-enhanced chemical-vapor deposition has been employed in order to grow the multilayers on either crystalline Si or fused silica substrates. The selection of the substrate took into account the particular experiments (optical spectroscopy or transport investigation) that had to be performed on the samples. The selected number of bilayers was often 30, as it offers a large enough thickness for the solar spectrum photons to be fully absorbed within the multilayers. Both materials (oxide and carbide) presented a good performance when fabricated taking into account this parameter. We were able to show that the number of bilayers was low enough in order to prevent the waviness propagation through the multilayers. Furthermore, it has been shown that post fabrication H_2 passivation of both material systems eliminates the still present dangling bonds, involving an important increase of photoluminescence (PL) emission and the absorption edge, also providing a higher electrical conductivity. PL studies revealed that the optimum annealing temperature is 1150°C for silicon rich oxynitride (SRON)/ SiO_2 multilayers and 1100°C in case of silicon rich silicon carbide (SRC)/ SiC multilayers, presenting the strongest emission intensity. A high crystalline degree of both systems annealed at their respective temperature was proven by Raman scattering. Quantum confined properties are strongest for the SRON matrix whereas in case of SRC and SRN matrix the optical and electronic properties are strongly influenced by defects even after hydrogen passivation.

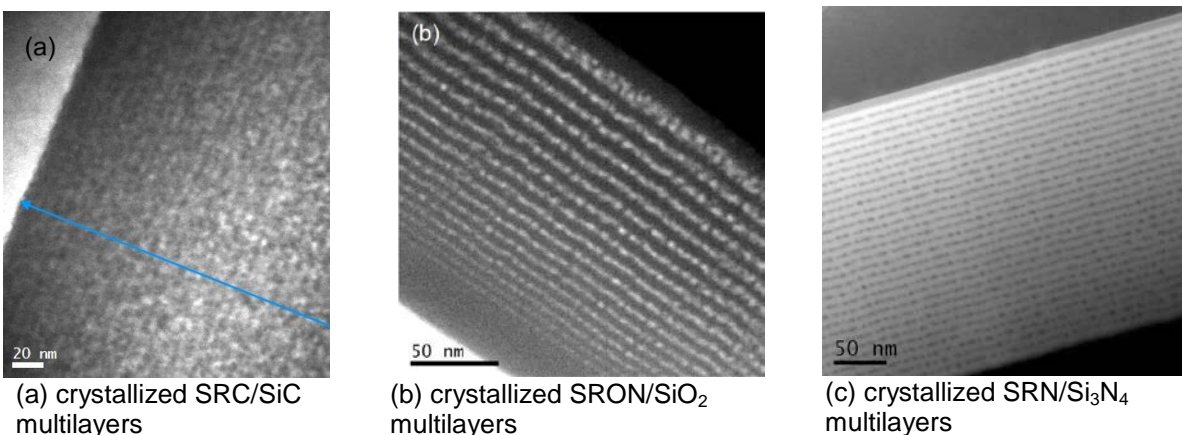


Figure 1: Successful fabrication of Si NCs containing multilayers offering size, density and barrier thickness control shown on selected examples for the different matrix materials.

Another crucial parameter for the fabrication of optimum multilayers is the thickness of the barrier layers, whose selection depended on different criteria with respect to the matrix material. In the case of SRON/SiO₂ systems, vertical electrical studies revealed that the conductivity increased several orders of magnitude if reducing the barrier thickness down to 1 nm, which is due to the enhancement of hopping probability between consecutive NCs. Regarding SRC/SiC systems, it was found that the multilayers underwent a severe shrinkage during the post annealing due to hydrogen evolution and crystallization, associated to the Si and C interdiffusion. Hence, a thicker barrier such as 6 nm barriers could solve this problem. This barrier thickness also increases the absorption of the whole structure for large photon energy, as stoichiometric SiC is a semiconductor with a band gap of about 2.5 eV. SRON/SRC/SRN layers are used establish the size controlled Si nanocrystals. In all three matrix materials we were able to fabricate the respective size controlled Si nanocrystals; however for the SRN material the samples did not behave as expected from quantum confinement and were excluded from further consideration.

Optical absorption and PL studies revealed a proper band gap energy for SRON layer thicknesses of around 3 – 4 nm. Electrical results showed increasing conductivity at thicker SRC layers. Moreover, absorption measurements stated that SRC layers thicker than 2 nm gave increasing absorption edges above 2 eV. For these reasons, we considered 3 – 4 nm as the optimum SRC thickness range for the SRC material. Many different Si excesses were employed within the first half of the project. In the case of SRON/SiO₂ systems, electrical results showed that x values (from SiO_x) lower than 1 (such as 0.85 or even 0.64) implied an important increase in the multilayer's vertical conductivity. However, due to difficulties in deposition control of such Si excesses, x = 1 was selected as the optimum composition for the sake of the project aims. In addition, this composition presented good crystallization and emission properties. The composition of SRC/SiC multilayer systems was more complex to select. We studied x values (from Si_xC_{1-x}) of 0.6, 0.65, 0.75 and 0.95. After the annealing process, the multilayer structure was only held in samples with a very high Si excess (x = 0.8) and with 3 – 4 nm SRC layer thicknesses, whereas at lower x values and thinner SRC the superlattices were lost. We finally decided to fabricate samples with x = 0.9, as this material presents a proper band gap energy, high absorption and good electrical conductivity. The SiC thickness larger than 3 nm (after annealing) was also found to be mandatory to control the nanocrystal size.

Table 1: Summary of the optimum parameters for the two different material systems studied within the NASCEnt project.

Parameter \ Material system	SiO _x /SiO ₂	Si _x C _{1-x} /SiC
Number of bilayers	30	30
Annealing temperature	1150 °C	1100 °C
Barrier layer thickness	1 nm	5 nm
Si-rich layer thickness	3 – 4 nm	3 – 4 nm
Si-rich layer composition	x = 1	x = 0.9

After these extended material optimizations, the next step was the realization of doped multilayers. The doping process was chosen to be during the deposition which offers the advantage of a selective doping of the layers. However, the longtime annealing process needed for crystallization could also lead to a redistribution of the dopants. In addition, especially doping for Si NCs is discussed controversially in literature; hence our results are

a mandatory step to a better doping control and understanding. In a first step for the SRON quantification of the phosphorus doping within the layer were monitored by SIMS.

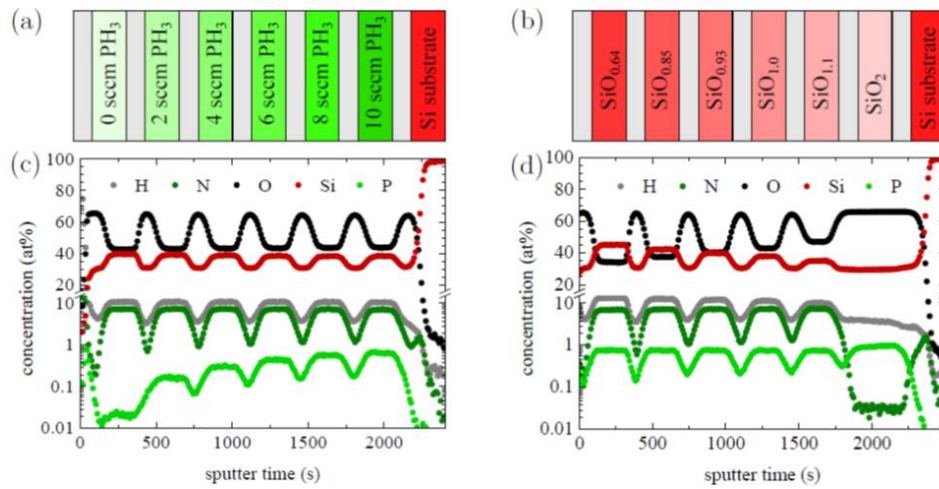


Figure 2: (a) increasing P doping with increasing PH₃ flow, and (b) influence of the SRON stoichiometry on the doping efficiency.

We found that the P content of the SRON layers depends linearly on PH₃ flow and is independent of stoichiometry. The localization of the dopants was investigated by XPS, XANES and atomic probe microscopy (APT). We found evidence for P within the Si NCs but also a segregation of the P at the Si/SiO₂ interface. The respective results are in the process of publication.

In case of the SRC/SiC multilayers a remarkable diffusion of dopants was observed. Comparison with bulk values suggests diffusion enhanced by SiC grain boundaries. Impurities diffuse rapidly along the SiC grain boundaries, but not into the grains. In spite of the diffusion the electrical properties of the multilayers with P doping are practically unchanged if only the SiCN are P doped. Fig. 3 demonstrates the P diffusion detected by FTIR.

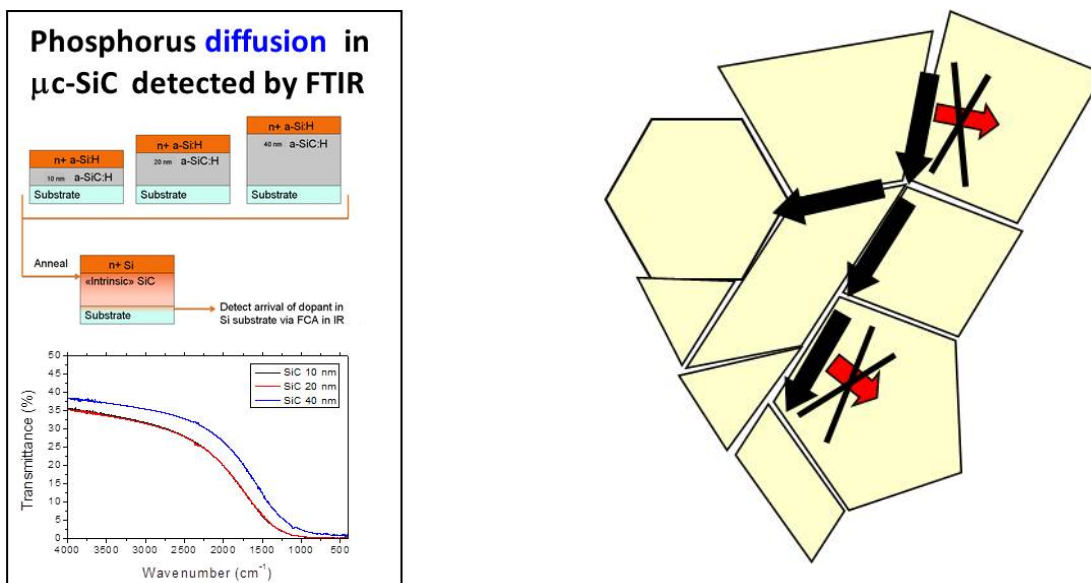


Figure 3: (a) FTIR results, showing free carrier absorption in the substrate (b) grain boundary diffusion.

The results demonstrate that modulated doping can be applied to the SRC/SiC multilayers. The presence of doping impurities was also detected not to affect the silicon crystallization process (see Fig. 4) and to enhance the PL signal. In summary, doping of SRC/SiC multilayers allowed to achieve remarkable conductivity and ohmic transport, which guarantees the minimization of series resistance in the devices. The electrical properties of SRC/SiC multilayers are reported in Fig. 5.

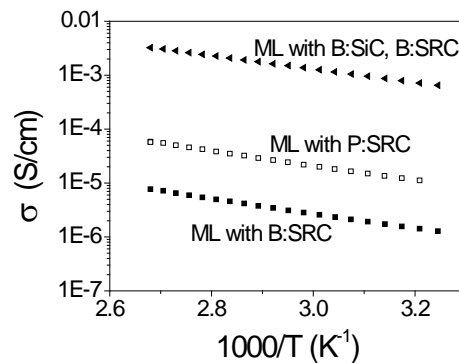
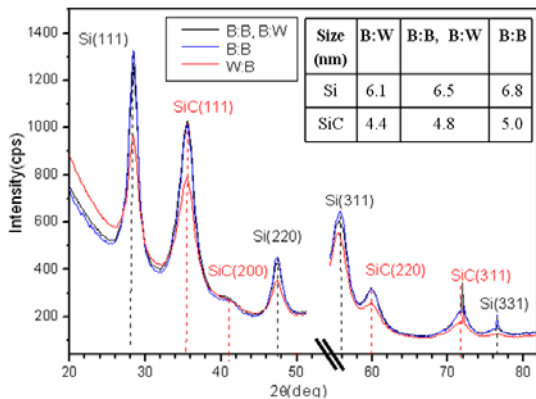


Figure 4: Diffraction spectra of doped SRC/SiC multilayers, illustrating the nanocrystal formation.

Figure 5: Electrical properties of doped SRC/SiC multilayers.

In the last period of WP 2 the thermal budget was investigated to fit better to technological needs such as back and top cell configurations. The normal longtime annealing could cause a significant diffusion of the dopants; hence destroy the required device structure of the solar cell. In principal temperatures in the range of 1000°C cannot be avoided if Si nanocrystals are used in the quantum structure. But time can be reduced for the SiO phase separation and crystallization can be accomplished on sub-second timescales if using rapid thermal annealing (RTA) or flash lamp annealing (FLA). However, pure short time annealings result in very weak PL due to the remaining high P_b -defect densities. The best way would be the combination with long-term & medium-T post-annealings and H_2 -passivation to improve the PL. Please note, there is a trade-off between thermal budget and Si NC quality as can be seen in Fig. 6.

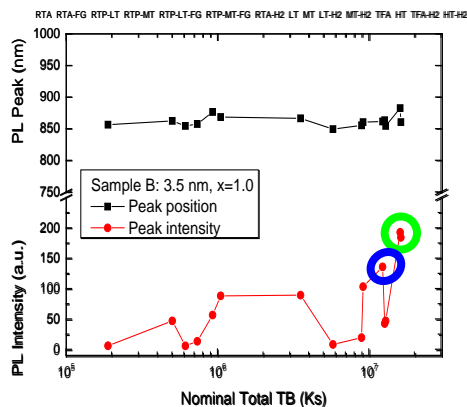


Figure 6: Comparison of PL peak position and PL intensity as a function of the nominal total thermal budget.

Similar results were obtained from experiments on thermal budget reduction in SRC/SiC. We have shown that a high crystallization fraction requires sufficient annealing time, however, the increase of annealing temperature from 1100°C to 1150°C allows to cut the annealing time down to 2 minutes with only moderate drawbacks on the crystallized fraction, which indicated the route of RTA to produce the desired material. Again a trade-off is needed for minimized thermal budget and nanocrystal quality. The occurrence is illustrated in Fig. [7]

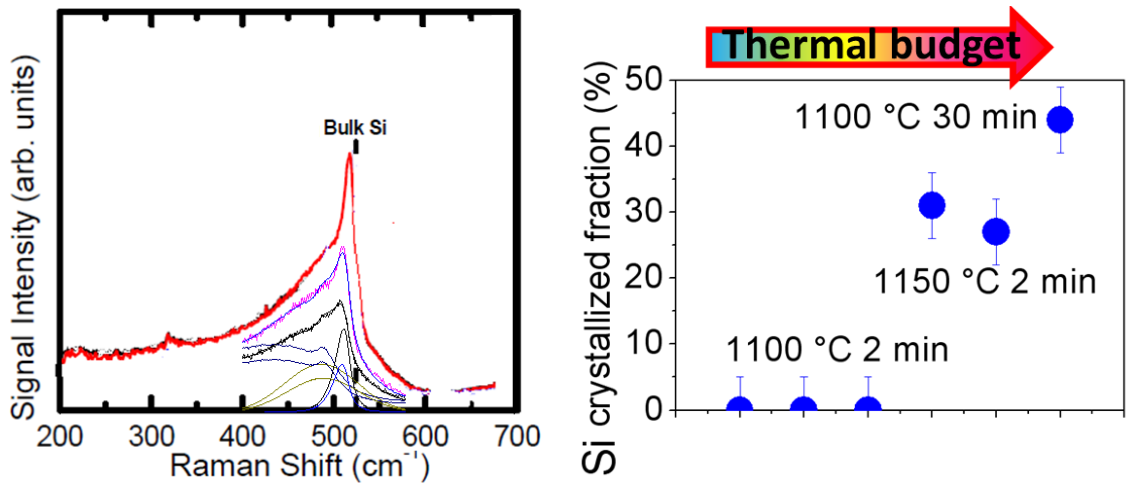


Figure 7: Thermal budget reduction in SRC/SiC. (a) Raman spectra, illustrating the crystallized fraction. (b) Crystallized fraction after thermal treatments.

Based on the above results the following conclusions can be drawn for application of Si NCs in solar cell devices. Embedding the Si NCs in SRON matrix has the advantage of a good size control, a very high crystallinity and a low defect density. The multilayer structure shows a medium absorption and a low conductivity due to the high band gap of the SiO₂ matrix material. Doping is not trivial but manageable. For the case of the Si NCs in SRC matrix we also established a good size control and high crystallinity. However, size control and crystallinity depend on each other and the material has an overall higher defect density, which implies some contribution to light absorption from the SiC matrix. Increased absorption is however also detected in the SRC, with direct impact on the design of the solar cell device. The specific advantage of the material is the high conductivity values due to the SiC matrix. In addition, the doping of matrix and quantum dots is much easier.

WP3: Theoretical Studies and Modelling

Task 1: Si/SiO₂, Si/SiC and Si/SiN_xO_y systems: theoretical data [Unimore]

This task is referred to the milestone MS4 and to the deliverable D.03.1.

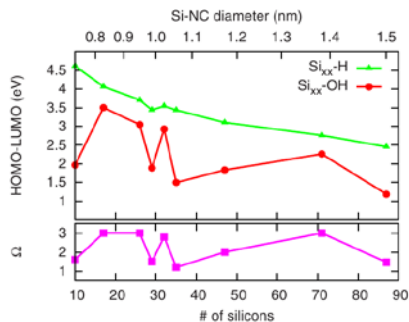


Figure 8: HOMO-LUMO gap of H-(green) or OH-(red) terminated NCs as a function of the size. Purple curve express the oxydation (hydrogenation) degree, i.e. the average number of H or OH passivant per interface Si.

We have developed and performed ab-initio computational methods for determining the structural, electronic and optical properties of Si nanostructures. We have concentrated our interest to those nanostructures that play a role in photovoltaic applications. In particular, we presented one-particle and many-body results for freestanding and embedded Si nanocrystals. The obtained results shed light on the importance of ab-initio calculations in systems of reduced dimensionality in order to elucidate quantum confinement effects. In all cases a comparison with the available experimental data, in particular with those produced within our projects has been performed. In particular we showed for Si NCs

embedded in oxide matrices how the absorption threshold depends both on the size and the oxidation degree. Besides, we have clarified the role of crystallinity and amorphization and through the calculation of recombination rates and absorption properties we have highlighted the best conditions for technological applications. The analysis of the results for the embedded NCs reveals a clear picture in which the smallest, highly oxidized, crystalline NCs, belong to the class of the most optically-active Si/SiO₂ structures, attaining impressive rates of less than 1 ns, in nice agreement with experimental observations. From the other side, a reduction of five orders of magnitude (10 ms) of the emission rate is achievable by a proper modification of the structural parameters, favouring the conditions for charge-separation processes. Moreover the role of nanocrystal-nanocrystal interaction has been investigated showing that the NC-NC interaction can be considered as an additional parameter (tunable by the NC density) that concurs to the characterization of the system behaviour: while the NC-size primarily determines the absorption/emission energy, the interaction level affects the absorption/emission rates. This picture opens to the possibility of creating from one side (high rates) extremely efficient Si-based emitters, and from the other side (low rates) photovoltaic devices capable to harvest the full solar energy with high yields.

The major drawback of using SiO₂ is related to its dramatic energy gap. Alternative materials like silicon carbide (SiC) or silicon nitride (SiN_x) have been proposed recently as possible substitutes for SiO₂ in hosting NC in PV solar cells.

In the case of the Si/SiN_x systems our results support the hypothesis that the photoluminescence of a-SiN_x samples is due to states associated to Si-N-Si bridge bonds at

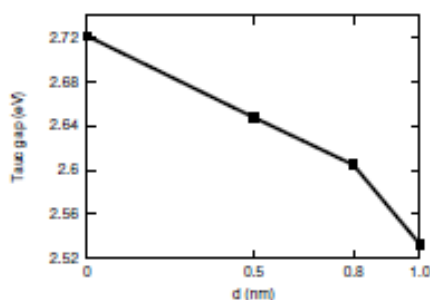


Figure 9: Tauc gap as a function of the size of the SiN_x embedded Si-NCs. The gap value of the pure a-SiN_{1.33} matrix is also reported and denoted by d = 0.

the nanocrystal/matrix interface. In fact, the number of such bonds, and the associated states, increases with the size of the nanoparticle and the PL intensity grows accordingly, at least in a limited range of d. The small dependency of the PL on the NC size seems to indicate that H-free samples containing NCs are less suitable for producing Si-based emitters, while the possibility of tuning the optical absorption energy might be exploited in PV applications.

Finally for the Si/SiC systems our calculated band structures for embedded nanocrystals of different size

show a significantly reduced quantum confinement effects, where the larger NCs show band structure characterized by states with some dispersion in energy. The relaxation of the structures evidenced a rearrangement of the atomic positions in the proximity of the Si/SiC interface, due to the difference in the lattice constants between the embedding and embedded materials, showing the necessity to have a considerable amount of SiC material around the NC in order to promote their formation, as showed by the experiments in the project. These consideration must be counted when comparing the above result with experimental observations. Moreover our results indicate an improved charge transport capability with respect to the silicon dioxide case. Also, the positioning of the NC states indicates the possibility of a type II band-offset, suggesting the possibility of enhancing the spatial separation of the electron-hole pair.

Task 2: Doping in Si/SiO₂, Si/SiC and Si/SiN_xO_y systems: theoretical data [Unimore]

This task is referred to the milestone MS4 and to the deliverable D.03.2.

While the use of doping to tune the conductivity of bulk silicon is widely practiced, its employment in Si-NCs is strongly linked to the knowledge of the real position of dopant species in the matrix embedded systems.

As starting point we have calculated the most probable localization for n- and p-type impurities in the Si/SiO₂ system. The following figure (where red and green curves are associated to phosphorous and boron doping, respectively) display the difference in the total energy for the samples with a single dopant placed:

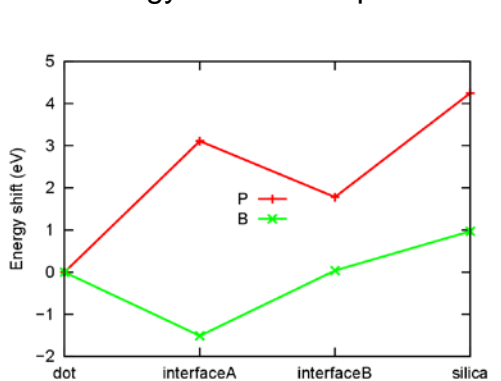


Figure 10: Total energy shift calculated for the 1 nm sized Si-NC embedded in SiO₂ doped by either P or B atoms placed: at the NC center (dot), at the Si/SiO₂ interface connected to 3 O atoms (interface A), at the Si/SiO₂ interface linked to 1 O atom (interface B), in the SiO₂ matrix far from the NC (silica). The zero in the figure is related to the total energy calculated for the dopant atom

in the NC (dot), at the interface bound to three O atoms (interface A) or to one O (interface B), in the silica far away from the NC. In every case, for both impurities, the NC is better than the silica matrix, however B prefer to stay at the interface, whereas P like to be in the NC. These results strongly depend on the doping-type, since the same outcomes is produced for As and N atoms and is linked to the electronegativity of the dopant species. The influence of these results on the optoelectronic properties have been evaluated and originate absorption peaks within the band gap of the undoped Si NCs.

Through our results related to total energy calculations and to the optoelectronic properties, discussed and favourably compared with the experimental outcomes, for all the considered systems, we can conclude that:

- i) it is easier to dope larger Si NCs, since for smaller ones there is a sort of self-purification effect, that tends to expel from the NC the dopant atom
- ii) in all cases, H or OH-terminated freestanding Si NCs and in SiO₂ embedded Si NCs, the P atoms prefer to stay in the core of the Si-NC, whereas B atoms like to be located near and at the interface of the Si NC;
- iii) due to the different opportunities for impurity localization usually the experimentally detected B concentrations are higher with respect to the P ones;
- iv) within the matrix, substitutional doping is energetic quite costly, consequently in the matrix an important role for dopant location is played by defects and dangling bonds;

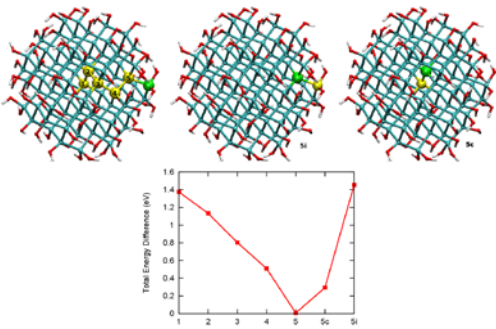


Figure 11: Top: OH-terminated Si₈₇ NC codoped by phosphorous (yellow) and boron (green). Bottom: The DFT total energy is plotted as a function of the P-B distance (1-5) and of the position of the pair for the smallest distance (5,5i,5c), as shown in top panel.

v) since similar conclusions are, at the present stage of studies, obtained for doped Si-NC embedded in silicon nitride and in silicon carbide, it seems general that in all matrix embedded systems it is possible to dope directly the NCs and that in order to improve the optical properties it is necessary an hydrogen treatment, which reduces the defect density; and that the defects related states play a significant role in the transport properties;

vi) in agreement with experimental outcomes we have proposed a structural model that show how pairs of P and B atoms in the sub-surface of Si-NCs play a crucial role for inducing negative surface potential in Si-NCs, thus rendering simultaneous doping of P and B an essential condition for the high dispersibility of colloidal Si NCs.

Task 3: Transport property simulation and recombination mechanism [Unimore-UB]

This task is referred to the milestone MS4 and to the deliverable D.03.1.

Within this task, we have presented a series of calculations in order to have a direct link between theory and experiment. In particular:

i) Optoelectronic Properties of of ensemble of embedded Silicon NCs: A model calculation has been developed in order to use the ab-initio results from single matrix isolated Si NCs as input for the determination of the absorption and emission properties of ensemble of nanocrystals. First, by performing DFT calculations on a set of Si-NCs, either passivated by H or OH, we have demonstrated the possibility of simulating the optical absorption

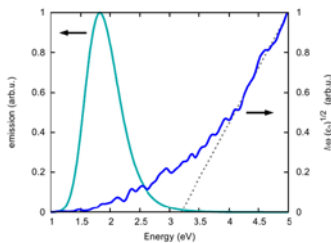


Figure 12: Optical emission (left curve) and absorption (right curve) spectra of OH-terminated NC ensemble with radius distribution parametrized. The Tauc fit is reported by the dotted curve.

spectrum of a set of NCs with a realistic distribution in the size. The calculated spectrum is validated by a comparison with the experimental absorption of a corresponding sample. Second, a purely-analytical model for the optical emission of NC ensembles has been parametrized by the DFT calculations and has been successively validated using experimental samples made by NCs with average radiuses of 1.1 nm and 1.7 nm. The presented model takes into account the oxidation degree of the NC, that appears particularly important for correctly describing the emission of the small NCs in the ensemble. Also, the important role of the SiO₂-induced stress has been confirmed, especially on the absorption, while a marginal role of the NC-NC interaction is deduced by the comparison with experiments at no too large NC packaging. The obtained results for the absorption and emission spectra of Si NCs that are in good agreement with the experimental outcomes enabling the evaluation of the best experimental conditions regarding PL results.

interaction is deduced by the

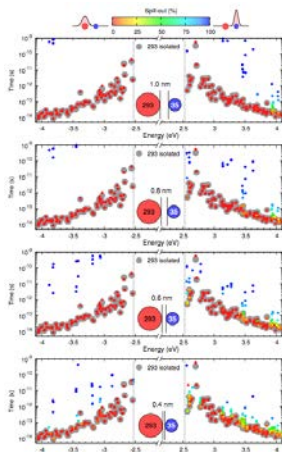


Figure 13: Calculated CM lifetimes for system formed by couple of interacting NCs.

ii) Recombination mechanisms in isolated and interacting nanocrystals: Carrier multiplications effects and multiple exciton generation. During the project we have developed a new highly parallelized code in order to calculate both Auger recombination (AR) and Carrier Multiplication (CM) processes in k-dispersive and nanostructured systems. In

particular, in the first part of the project, we have implemented a set of new routines for the calculation of AR lifetimes in semiconductors. In the second part of the projects, such routines have been modified to calculate CM lifetimes in low dimensional nanosystems, and in particular in silicon nanocrystals. Our results indicate that one-site, involving the single NC, mechanisms are always faster than two-site events, that involve more NCs. To find the conditions that maximize two-site carrier multiplication processes we have monitored their dependence on NC proximity and wavefunction's spill-out parameter. It is possible to observe that two-site lifetimes are larger when the spill-out is either 0% or 100%, that is, when the initial wavefunction is strongly localized onto one single nanostructure. In contrast, even a small delocalization of the initial wavefunction on both nanostructures is able to push up two-site Coulomb matrix elements. We observe changes of up to two to three orders of magnitude in lifetimes when initial state ceases to be completely localized on one NC and at least the 15% of the wavefunction is shared by the two NCs. The most efficient two-site events are recorded when the initial carrier wavefunction extends to both NCs and the spill-out parameter ranges from the 15% to 85%, which define the so-called wavefunction sharing regime. These results enable us to envisage the possibility of using the NC's density as a tool to improve carrier multiplication effects and multiple exciton generation.

iii) Transport Properties of embedded Silicon Nanocrystals. The results of ab-initio calculations of the electronic properties of embedded Si-NCs performed at Unimore have been used as input for a transfer matrix formalism developed at UB. The role of size, amorphization, matrix barrier height, doping on electron and hole transport has been elucidated. The results have been compared with experiments. Electronic transport is

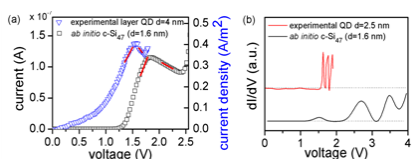


Figure 14: a) Comparison between an exp. I-V characteristic (blue triangles) of a layer of QDs of diameters around 4 nm and computed I-V characteristic (black squares) of one QD of 1.6 nm. Red lines are the slope of our curves. b) Comparison between an experimental dI/dV curve (red line) of one QD of diameter around 2.5 nm and computed dI/dV curve

of one QD of diameter around 2.5 nm and computed dI/dV curve of one QD of diameter around 1.6 nm. In a general trend, when diameter increases, the valence band offset (VBO) increases (the conduction offset, CBO, has a weaker dependence) and E_g decreases as well, with some fluctuations related to oxidation degree at the interface and to the strain induced by the embedding matrix. The number of states inside the barrier increases with the NC size. Thus, when diameter increases, the higher density of states and lower E_g enhances the current, whereas the higher band offset decreases it. Thus electron transport is enhanced in big systems because CBO does not vary significantly and E_g is lower for bigger systems. However, hole transport is enhanced in small systems because in this case VBO strongly depends on NC diameter, being lower for smaller NC and ruling over the other parameters. Concerning the systems morphology, amorphous NCs present higher electron current than crystalline ones for a given NC size because of their smaller E_g . Hole transport, however, is enhanced for crystalline systems due to the much smaller VBO, supporting the idea of an efficient electron confinement in crystalline NCs. Regarding the doped systems our results show that in the case of B doping the hole transport is enhanced, whereas electron transport is favored in the case of P doping as, also, showed experimentally within our project. Thus, our calculations show that the transport properties of Si NCs embedded in SiO_2 layers are sensitive to the microstructure of the NC/matrix interface. In practice, this means that the design and fabrication of devices based on NC with predictable properties requires a control of these properties that go far beyond the mere control of the NC diameter.

From all the previous theoretical results it is possible to derive general conclusions that can be of help to the experimentalists in order to move towards the optimal conditions for Si nanostructures based photovoltaic devices

Size: Optimal sizes: 2-3 nm in diameter, gaps in the right energy range and possibility of an high density of NCs.

Density: High density favours energy transfer, transport and recombination mechanisms such as carrier multiplication and multiple exciton generation.

Matrix: SiO₂ pro: stability, less number of defects, high NC density; contra: high band offsets, SiN_x pro: low band offsets; contra: large number of defects, SiC pro: tuneable band offsets; contra: stability, difficult NC size control

Doping: pro: enhancement of transport properties: holes and electrons, pro/contra: co-doping with B and P (tuning of PL vs Transport)

Transport: pro: doping, high density (formation of minibands), pro: positive role of defects or doped atoms in the matrix (ladder effect).

WP4: Electrical and Optical Properties of Multilayered Test Structures

Work Package (WP) 4, entitled “*electrical and optical properties of multilayered test structures*”, aimed at developing and optimizing test devices (*p-i-n* and MOS structures), employing Si NC multilayers as active medium, for their use as top cell of a tandem solar cell device. Different matrices based on SiC or SiN_xO_y were used for containing the Si-nanoprecipitates, each matrix providing them different electronic properties.

Basic test devices were proposed for being fabricated for assessing the optical, electrical and electro-optical properties of Si NCs inside either SiC or SiN_xO_y (which included optical absorption, carrier generation and recombination, trapped charge and electrical parameters of the devices). Consequently, an exhaustive characterisation was performed, allowing for determining the optimum electro-optical parameters for the final tandem cell.

This WP4 is divided into three different tasks, focused on different aspects of the device design and properties:

- 4.1. Design and fabrication of the test devices**
- 4.2. Optical properties of fabricated devices**
- 4.3. Electro-optical characterisation of the test devices**

Within task 4.1, different test devices were proposed for fabrication by using the best absorber Si NC layers in agreement with results obtained within WP2. In Fig. 1 we present a sketch of the cross-section view of the two devices that we considered: Fig. 1(a) for determining lateral and Fig. 1(b) vertical electrical properties. A considerable number of device runs were fabricated, considering Si NCs embedded in either SiC or SiO_xN_y matrices.

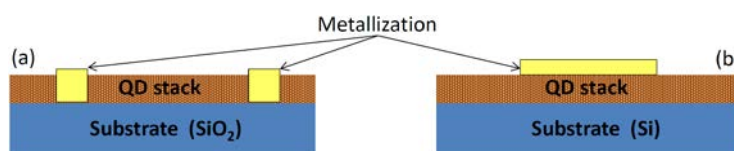


Figure 15: Sketch of test devices for their electro-optical characterization: (a) lateral and (b) vertical configuration.

In the initial device runs, the contact material and processes were optimized, finding good adhesion for Al and ITO with an ohmic $I(V)$ characteristic, materials that were employed for lateral and vertical devices, respectively. Because a high annealing temperature was required for precipitating the Si in excess into Si NCs, all the fabrication processes needed to be adapted to this requirement.

In the following runs based on the two matrices (SiC or SiN_xO_y), non-stoichiometric layer thickness (i.e. Si NC size), barrier thickness, stoichiometry and annealing temperature were varied in order to determine the best structural parameters in terms of transport and optical absorption. Please note also the different substrate that we employed for each kind of devices: an insulator and transparent SiO₂ substrate and *p*-type Si substrate for horizontal

and vertical configurations, respectively. Therefore, these structures allowed us determining the absorption coefficient of the active layers and, also, their emission properties.

In fact, a detailed knowledge of light absorption in our investigated multilayers and devices is essential for building the tandem solar cell devices:

- Knowledge of the optical gap
- Estimation of nanocrystal absorption cross-section (to calculate excitation rate etc.)
- Information on sample morphology and composition
- Understanding of the role of quantum confinement, local field effect, etc.

In addition, our Si NCs should present some optical properties to be implemented as a top cell of a tandem solar cell system: the optimal band gap of the top cell in a two-cell tandem (with a bulk Si bottom cell, $E_g \sim 1.1$ eV) is calculated to be between 1.7 and 1.8 eV, and the absorption coefficient above this band gap should be as high as possible in order to harvest light efficiently without necessity to grow very thick layers (or very high number of multilayers).

Using the devices in lateral configuration for developing task 4.2, we have performed an exhaustive optical characterization (absorption and emission) to determine the best structural configuration for achieving high absorption and large life time of photo-excited carriers, required for our proposes.

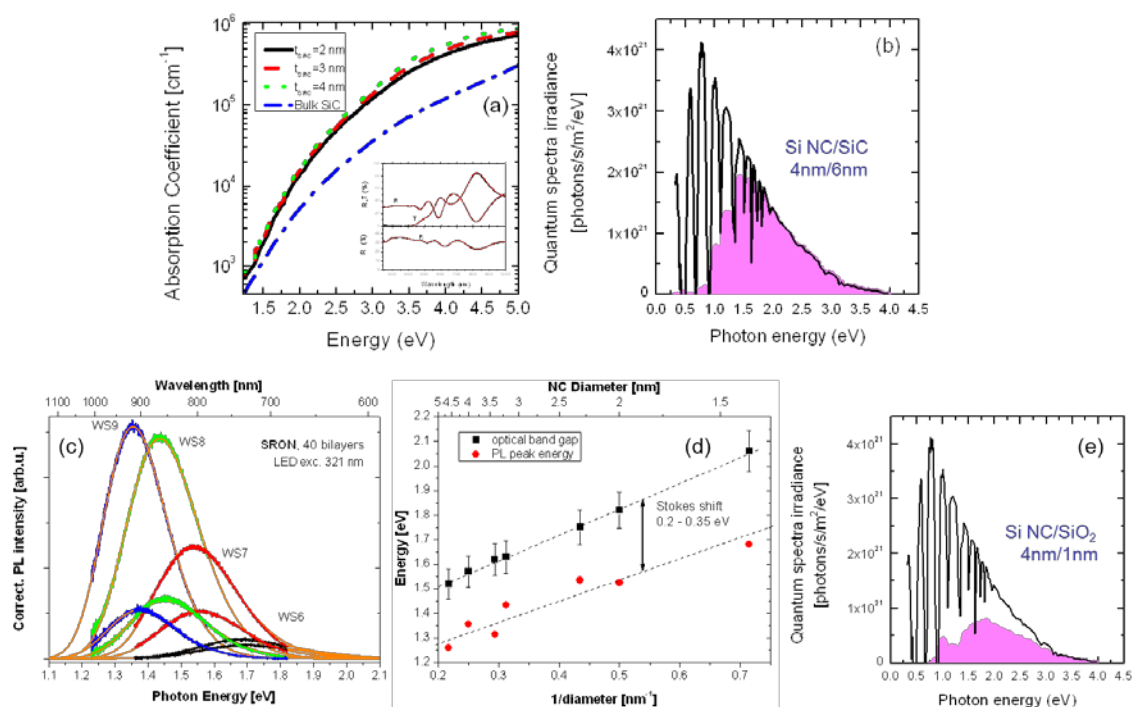


Figure 16: (a) Absorption coefficient of Si NCs embedded in SiC. (c) Photoluminescence emission of Si NC embedded in SiO₂. (d) Comparison between the emission energy and absorption edge energy for Si NCs embedded in SiO₂ of different sizes. (b) and (e) present (in pink) the region of the solar spectrum absorbed by Si NCs embedded in SiC or SiO₂, respectively.

Transmittance and reflectance measurements in samples with transparent substrates [devices with the configuration shown in Fig. 16a] allowed determining the absorption

energy edge for each Si NC size [see Fig. 2(a) and red dots in Fig. 2(d)]. In the case of Si NCs embedded in SiO₂, they present strong photoluminescence emission, making this technique suitable for analyzing their emission properties [see Fig. 2(c) and black squares in Fig. 2(d)], which is closely related to the absorption edge energy. Thus, both kinds of technique are useful for determining the optimum Si NC size for having an absorption edge around 1.7 eV: between 3 and 4 nm in diameter for both SiC and SiN_xO_y matrices. Moreover, the determination of the absorption coefficient in both systems is fundamental to evaluate the region of the solar spectrum absorbed by Si NCs [displayed in Fig. 2(b) and Fig. 2(e), in pink]. This way, it was found that an important absorption for energies above 1.7 eV is achieved by Si NCs embedded in both SiC and SiO₂ matrices.

The annealing treatment has also been highlighted as a crucial parameter, as high thermal budget produces the precipitation of highly crystalline Si nanoprecipitates. In fact, temperatures between 1100 and 1150 °C allowed their precipitation with excellent crystalline degree (around 80%). Larger temperatures produce the detriment of the multilayers, losing control on the Si NC size.

The stoichiometry and also the barrier thickness were other two parameters that strongly influence the precipitation process at the employed annealing temperatures. Thus, for keeping the multilayers structures and, trying also to increase as much as possible the volumetric density of Si NC, a stoichiometry of $x = 1$, $y = 0.23$ (SiO_xN_y) and $x = 0.85$ (Si_xC_{1-x}), for SRON and SRC systems, respectively, were found to be the preferential ones.

The aim of the final task within this WP4 was optimizing and determining the electro-optical properties of the test devices with the best structural and optical properties. Detailed current-voltage $I(V)$ electrical measurements under dark conditions were performed in all devices. Different problems were found in the initial devices, related to unintentional oxidation of the layers, parasite resistances, cracks in contact or bad adhesion, which strongly influenced on the electrical transport through the Si NCs and, thus, extracting unreliable information of their conduction properties.

The last set of devices, fabricated using the optimized Si NCs multilayers, overcome all the previous mentioned problems, displaying excellent structural and electro-optical properties. For this reason, these were the ones considered for the top part of the final tandem solar cell, being included in WP5. The electro-optical characterization of optimized structures is presented in Fig. 3. High current densities were obtained when devices are polarized in accumulation regime.

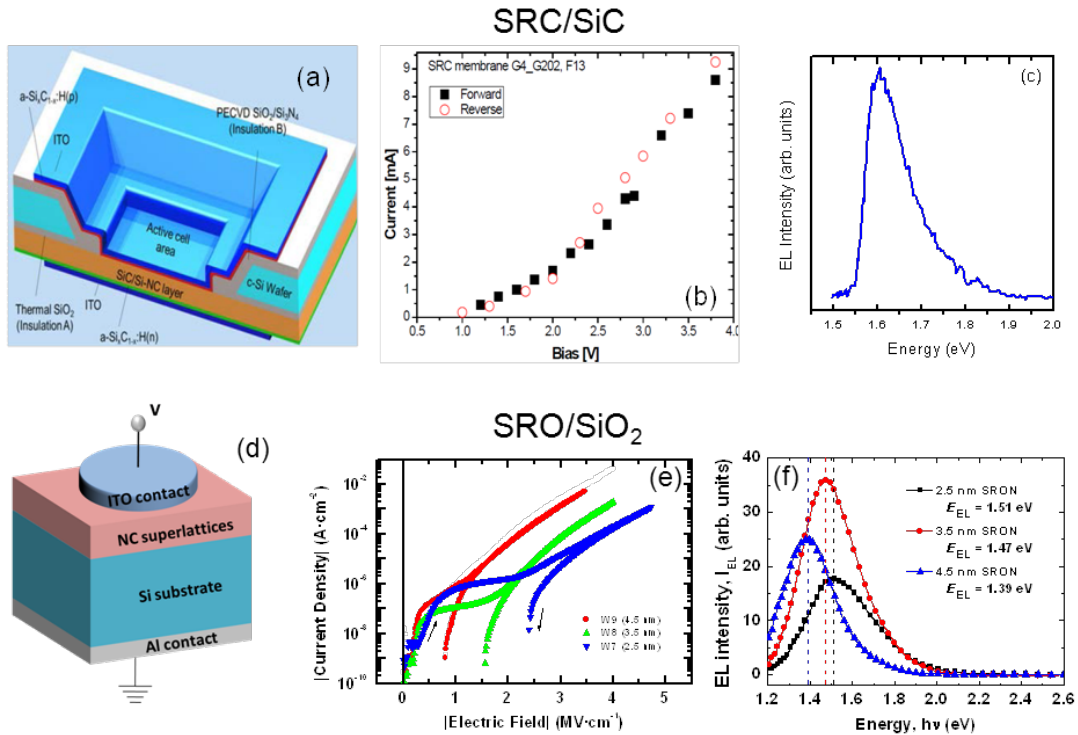


Figure 17: Scheme for a vertical p-i-n structure with a Si NC layer as the intrinsic region, embedded either in (a) SiC or (d) SiO₂. Current-voltage characteristics [(b) and (e)] of p-i-n structures and their electroluminescence spectra [(c) and (f)], for both SiC and SiO₂ matrices, respectively.

The $I(V)$ curves of the last set of devices [see Fig. 3(a) and (d)] allowed also to study the conduction properties of Si NCs as a function of the matrix and the Si NC size. In fact, we found that the conduction between Si NCs is mainly achieved by tunneling assisted by traps [see Fig. 3(b) and (e)]. So, the smaller the distance between Si NCs, the higher their interaction and, thus, the higher their conductivity.

The electro-optical properties of Si NCs were also assessed by means of electroluminescence measurements, revealing an intense emission at energies close to 1.7 eV for NC sizes between 3 – 4 nm [see Fig. 3(c) and (f)].

In summary, the studies performed within this WP4 have allowed determining the best structural parameters (see Table I) for optimizing the absorption and charge extraction in superlattices containing Si NCs in two different dielectric matrices, SiC or SiN_xO_y.

Table 2: Summary of the optimum parameters for the two different material systems studied within the NASCEnT project.

Parameter \ Material system	SiO _x N _y /SiO ₂	Si _x C _{1-x} /SiC
Number of bilayers	30	30
Annealing temperature	1150 °C	1100 °C
Nominal barrier layer thickness	1 nm	6 nm
Nominal Si-rich layer thickness	3 – 4 nm	3 – 4 nm
Si-rich layer composition	$x = 1, y = 0.23$	$x = 0.85$

WP5: Device Fabrication and Characterisation

Task 5.1: Proof of quantum confinement effect on solar cell device level

Quantum confinement in Si NCs embedded in SiO_2 has been shown optically by means of photoluminescence in many publications over the past 10 years [1-4]. However for a functioning solar cell that exploits this effect, merely showing quantum confinement optically is insufficient. There are a range of mechanisms that can occur within a cell that can cause the open circuit voltage to remain significantly lower than the band gap, such as bulk recombination, high series resistance, interface recombination at the contacts, surface recombination at free surfaces, or simply insufficient absorption to achieve the desired quasi-Fermi level splitting. Ultimately, if the open circuit voltage cannot be increased above that of a regular Si solar cell, then no exploitation of the quantum confinement effect occurs, which in turn is needed in order to use this cell to boost the overall efficiency in a tandem configuration. At the same time, because it is impossible to already have all the loss mechanisms listed above under control in the first set of NC solar cells that are produced, a comparatively modest open circuit voltage cannot be taken as proof that quantum confinement is not present on an electrical level.

A hetero-device, where the contacts are made of a different material than the NC layer, was chosen so as to be able to use well-known contact materials, reducing the number of unknowns in the final device structure. The device structure chosen is shown in Figure 19, and its processing explained in detail in Ref [5]. As all active layers other than the Si NC layer are formed after the annealing needed to produce the NCs, interdiffusion or any other reaction between the layers is minimised.

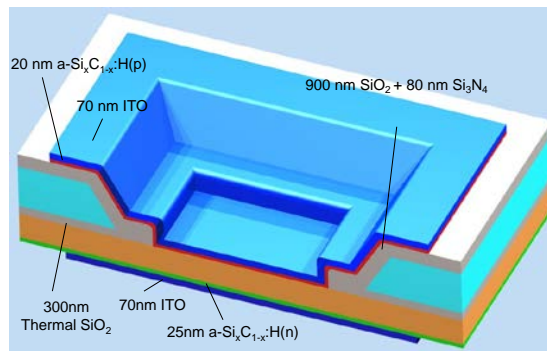


Figure 18: Device structure used for demonstration of quantum confinement on solar cell device level. Reproduced from [6]

The structure was realised at Fraunhofer ISE using Si NCs embedded in SiC. Solar cell results under various illumination levels are shown in Figure 2. The best cell exhibited an open circuit voltage of 370mV under 1 sun illumination [5], while that of another cell was increased from 282 to 450mV by concentration of incident light, increasing efficiency [6]. This is an impressive result considering it is measured on NCs embedded in SiC, a material that is known, both from work within the NASCEnT consortium and the literature, to be defect-rich, and on which unambiguous optical proof of quantum confinement is lacking. We therefore expect that the same structure produced with Si NCs embedded in SiO_2 should

have little problems in reaching higher Voc. This has thus far been hindered by the insufficient mechanical stability of the SiO₂-based membranes, related to the higher mechanical toughness of SiC as compared to SiO₂, however this issue can be resolved with further process development.

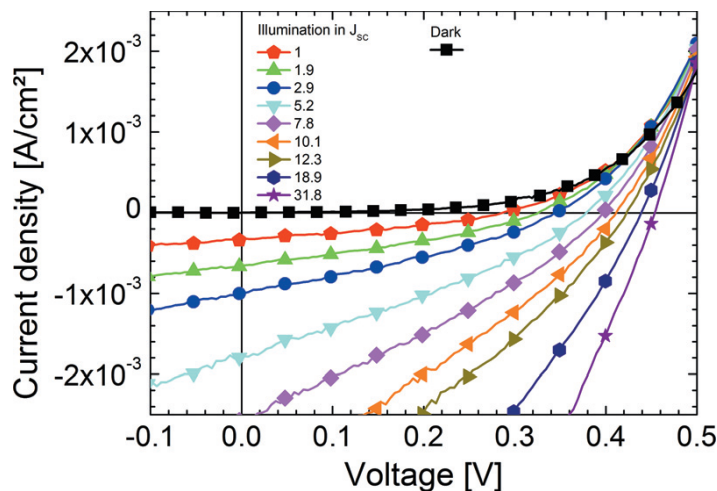


Figure 19: I-V curve of a solar cell with an absorber of Si NCs embedded in SiC. Open-circuit voltages of 282mV at 1 sun and 450mV under concentration are obtained. Figure reproduced from [6].

Task 5.2: Evaluation of technologies for p/n-junction, structuring and contact formation

In order to build an efficient solar cell, it is not only necessary to have good NC material, but also to add the different components needed for a cell in the best way possible. This requires p/n-junction formation, to permit charge separation without which no photovoltage can be developed; contact formation, without which no current can be extracted; and structuring, which is necessary as different areas of a cell must be assigned to the different functions required.

We found that any method that involves exposing one of the p- or n-layers to the annealing used to produce Si NC will not work, either because it involves a materials system in which dopants are insufficiently activated (poly-SiC, see Figure 21) [7], and/or because the degree of dopant diffusion into the Si NC film is too great.

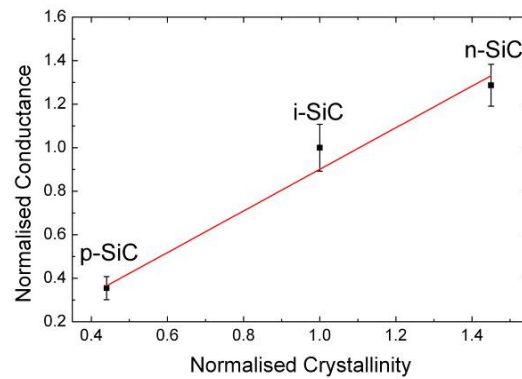


Figure 20: Conductivity of doped poly-SiC [8]. Conductivity is related to crystallinity; no electrical activation of dopants was observed. Reproduced from [7].

The latter can change the properties of the Si NC film itself, making it impossible to produce a structure in which the Si NC film can be investigated in the state in which it was intended to be produced. We have therefore decided that the most promising way of forming a p-n junction that permits rigorous characterisation of the photovoltaic properties of Si NC is to deposit p- and n-type $a\text{-Si}_x\text{C}_{1-x}\text{:H}$.

Having established that p- and n-type $a\text{-Si}_x\text{C}_{1-x}\text{:H}$ are the best way to form a charge-separating junction in an Si NC cell, we developed suitable structuring routes to create cells that utilise these materials in junctions with vertical transport through the Si NC layer. The creation of junctions with lateral transport through the Si NC layer is possible in principle but was not the subject of research within this project because minority carrier diffusion lengths were suspected to be less than the minimum feature size realisable in lateral configuration. Creating a vertical device where both p- and n- $a\text{-Si}_x\text{C}_{1-x}\text{:H}$ are deposited after Si NC annealing was tricky because the substrate must be locally removed and electrical contact to the substrate avoided at all costs, but such a device, termed a “membrane” device, has been successfully produced (see Figure 19). Structuring was done via low-cost inkjet printing of hotmelt resists (as compared to the much more expensive photolithography processes). The properties of the $a\text{-Si}_x\text{C}_{1-x}\text{:H}$, the interface pre-treatment, the inkjet printing process and the insulation layers have been optimised, and electrical characterisation has proven conclusively that the devices work in the way they are intended to [5, 9, 10]. We have also managed to correlate EBIC, LBIC and optical microscopy to greatly facilitate analysis of device failure, as shown in Figure 22 [11].

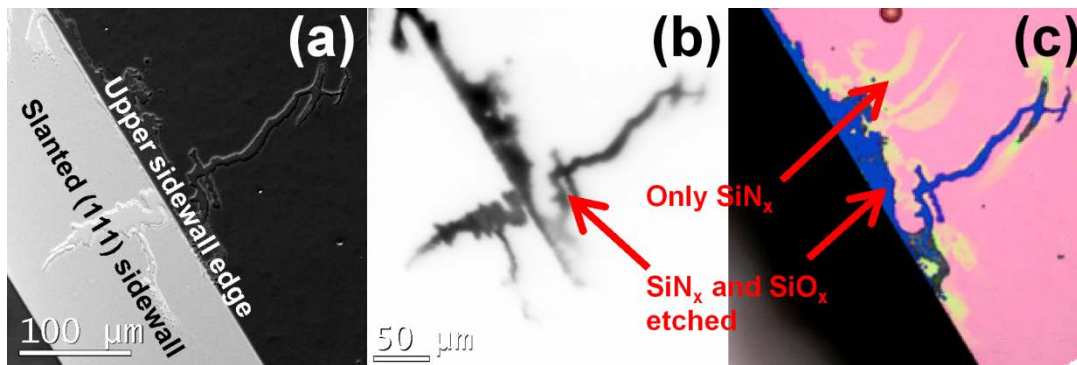


Figure 21: Scanning electron micrograph (a), electron beam induced current (EBIC) map (b) and optical micrograph (c) of a membrane cell shunt path. The clear correlation between EBIC and light microscopy will permit the accurate detection of shunts by light microscopy alone in future devices. Reproduced from [11].

Finally, we have tested a range of contact materials in order to reduce the effect of contact resistances and non-linearities arising from Schottky contacts on the electrical measurements of test devices and solar cells. We found Ti and NiCr to be best for SiC-based NC layers [7]. Joint work between IMTEK, STM and ISE showed that Al forms a good contact to devices from Si NC embedded in SiO₂.

Task 5.3: Development of tunnel diodes for high-temperature and middle-temperature route.

Tandem solar cells such as the one between nanocrystalline and bulk Si envisaged in this project are only economically viable if they are monolithically integrated. This means electrons flow from the n-region of one cell through the external circuit and recombine with the holes in the p-region of the second cell. For this to work, electrons in the n-region of the first cell and holes in the p-region of the second cell must be annihilated, either through recombination or interband tunnelling in a tunnel diode. Two methods are possible which come from the state-of-the-art in the interconnection of III-V multijunction cells and a-Si/ μ c-Si micromorph cells respectively. The former involves band-to-band tunnelling in a defect-free, degenerately doped p-n junction that exhibits negative differential resistance. This classical tunnel junction, which can withstand very high current densities, requires high material quality and abrupt doping profiles that are difficult to maintain during high-temperature tunnel diode anneals. A more reasonable approach is the latter, the tunnel recombination junction [12, 13], where the dopant profile allows the accumulation of electrons and holes near the junction, and tunnelling of carriers between the conduction band of one cell and the valence band of the other occurs via defects embedded in a defect-rich recombination layer at the junction. We produced such a tunnel junction from n+ poly-SiC and p+ poly-Si in the configuration shown in Figure 5 (left). As a particular test of resilience to thermal processing, the poly-Si was remolten on top of the SiC after deposition [14]. Despite this severe thermal budget, the device still exhibits Ohmic conduction with low sheet resistance above a certain critical SiC doping level, and the potential required to pass a typical tandem solar cell current density of $\leq 20 \text{ mA/cm}^2$ is negligible [15]. This indicates

that this kind of junction is suitable for the interconnection of an Si NC cell processed with high thermal budget and a conventional Si bottom cell.

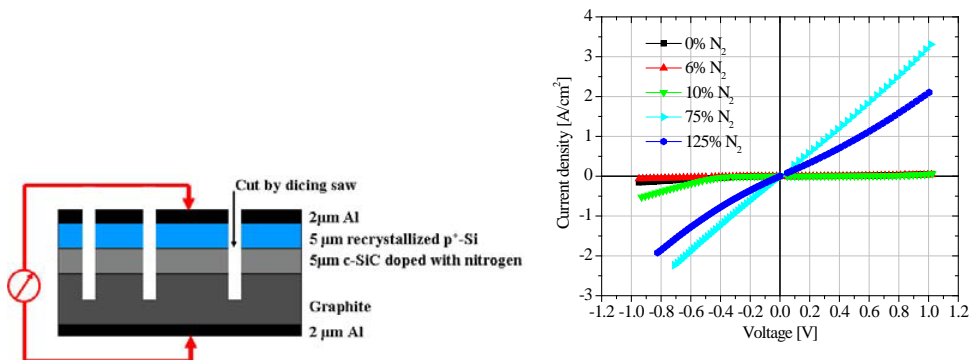


Figure 22: Test device structure (left) and IV curves for different nitrogen doping levels (right) of a n+ SiC / p+ Si tunnelling recombination junction. It can be seen that with sufficiently high doping, Ohmic IV curves are obtained, and the potential required to pass a typical tandem solar cell current density of $\leq 20\text{mA/cm}^2$ is negligible. Reproduced from [14] (left) and [15] (right).

Task 5.4: Tandem solar cell device simulation, fabrication and characterisation.

As mentioned previously, tandem cells are only economically viable when monolithically integrated, and one key requirement for this, aside from the tunnel junction described in Section 3, is current matching. If the two cells do not produce the same current, a field will develop in the “stronger” cell until its performance has been lowered to that of the “weaker” cell [16]. To avoid this, we have calculated the layer thicknesses we would need for a current-matched Si NC/SiC – $\mu\text{c-Si}$ tandem cell using the layer stack shown in Figure 6 (left) as a model system.

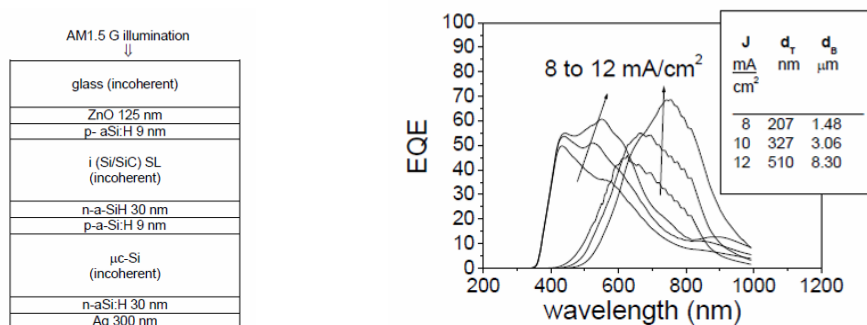


Figure 23: Structure of simulated tandem cell (left), calculated spectral response of top and bottom cells; thicknesses needed for given short circuit currents (right). Reproduced from [17]

The result that even thicknesses in the range of hundreds of nm are sufficient for current matching in the 10mA/cm^2 range is very encouraging as such thicknesses can be grown in a reasonable time by PECVD, the technique currently used for Si NC precursor deposition. This, along with the calculation of the conditions required for suitable quasi-Fermi level splitting in Si NC films [18], allowed us to progress onto the practical realisation of an Si NC tandem cell.

The structure of the tandem cells produced is shown schematically in Figure 7 (left). All the processes developed previously are employed here for optimum device performance, in particular the a-Si(p):H emitter, which had been shown to be preferable to doping the NC layer, and the n+ SiC / p+ Si tunnel contact [19].

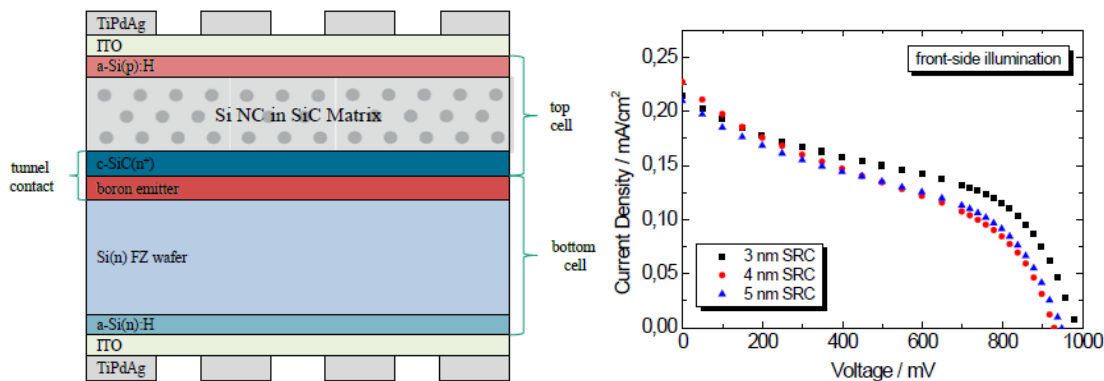


Figure 24: Structure of tandem cell produced (left), IV curves of cells with different nominal Si NC sizes (right). Figures reproduced from [19]

A V_{oc} of 900-1000mV was achieved, which is significantly higher than the maximum possible with an Si wafer and shows that the device produced is a fully functioning tandem cell. The V_{oc} is largest for the smallest nominal NC size, as one would expect from a quantum-confinement viewpoint.

Task 5.5: Cost calculation for crystalline Si wafer based (high-temperature) and superstrate (middle-temperature) tandem solar cell device.

In order to evaluate whether the Si NC tandem cell makes economical as well as scientific sense we performed a cost calculation using SCost [20]. The cell production cost per wafer was found to be 60-70% higher than for a conventional cell, leading to the requirement of 30% efficiency to offset the cell production cost. The key cost-driver is the time required for PECVD deposition of the Si NC precursor, which is assumed to be 5mins for this calculation. The annealing, which is the other additional process step, is not significant by comparison. Fortunately, the advantage of having higher efficiency is multiplied once material, module and installation costs are accounted for because it means fewer wafers, fewer modules and less land are needed. The efficiencies required for cost parity with conventional cells is thus reduced to 23%, 21% and 20.5% on cell, module and system level respectively. This means that once the costs all the way to the installation are accounted for, an Si NC tandem cell need only be a few percent more efficient than a conventional Si solar cell to be competitive in the market.

WP6: Dissemination and Exploitation

The work-package 6 was intended for organization of efficient dissemination of information on the project activities and achievements. Various ideas on exploitation of project results were collected throughout the project duration and resulted in the final *Technical exploitation roadmap*.

The initial activities concentrated on the realization of the first two milestones:

MS.13 – Starting basic project web site (M1)

MS.14 – Full working project web site (M6)

The official Web site was registered at the address www.project-nascent.eu immediately following the decision during the kick-off meeting and then the web-hosting was arranged and a basic page was designed.

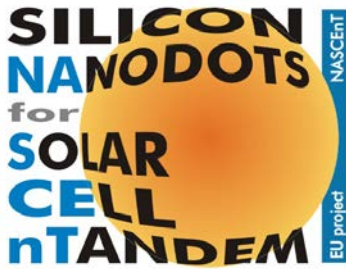
The complete web site was prepared and opened to public at the beginning of February 2011 - so, the two milestones were fulfilled in time.

During the project work the website was updated regularly and it will continue existing for more than one year after the end of project (till October 2014) in order to further disseminate the results of our work.

There was also an internal restricted-access part of the website, which enabled efficient exchange of internal information of the consortium. For example, information on sample batches fabrication and testing, meetings organization and project reports, working reports and publications under preparation or even external papers of special interest. We can conclude that the internal website substantially helped efficient management of the project (WP1).

Project logo

An internal “call” for logo proposals was initiated during the kick-off meeting. Four designs were submitted to the consortium voting. The distinct winner was a logo shown below, which was then used for project reports and presentations. The attractive design of the NASCENT logo effectively identified work done within the project especially at large conferences like E-MRS meetings.



D06.2 Organization of workshop “Nanostructures for solar cells with optimised solar spectrum usage”

The deadline of this deliverable was shifted by several months (from February to May) following the previous discussions and agreement. The reason was to find better dates for students (avoiding strong collision with teaching periods) and researchers (in relation to main conferences and meetings).

The project consortium decided that the best form of the workshop will be a tutorial connected to a bigger meeting in contrast to adding a separate event in the already busy list of conferences, meetings and schools.

As the big part of the solar-cell-materials research community used to attend the E-MRS spring meeting in Strasbourg we arranged organization of a tutorial session at the day before starting of the E-MRS meeting. The E-MRS head quarter gave us a room for this tutorial and advertised it on the E-MRS web site.

The tutorial took place on Sunday May 26th from 15 to 20 hours consisting of five long lectures covering the basics of solar cells, theoretical background of the group-IV nanomaterials, growth technology and characterization techniques and, finally, the application of nanostructures in devices. All lectures were presented by NASCEnt partners.

An electronic pre-registration was required in order to know roughly number of participants (for the adequate lecture hall size and refreshment capacity). We had 33 registered participants but many more just came in the hall during the tutorial. So, finally we get auditory of about 40-50 people.

Our tutorial session received quite positive feedback. The executive committee of E-MRS expressed intention to have more such tutorials in future.

D06.3 Proceedings of the workshop

The tutorial presentations were mostly based on the materials prepared for the book *Nanotechnology and Photovoltaic Devices: Light Energy Harvesting with Group IV Nanostructures*, which we started to prepare in summer 2012. The book to be published by

the Pan Stanford Publishing is edited by J. Valenta and S. Mirabella and also majority of contributions are written by NASCEnT partners. The book is oriented to students and newcomers in the field of nanostructures for solar cells. Currently, all chapters were revised and submitted to the publishing company and the book should be published early in the year 2014. We believe that this book will make a durable trace of the NASCEnT project in the PV development field by educating new researchers.

The scientific outputs of the NASCEnT project were presented in special symposia of the E-MRS meeting, mainly the *Symposium D: Advanced inorganic materials and structures for photovoltaics* (10 contributions and 3 presentations in other symposia) where one session was specifically devoted to NASCEnT presentations. Our project supported this symposium and our logo was presented on the web, and the printed programme. Papers from the presentation will be mostly published in *Energy Procedia* (open access) and accessible at the project website.

Publications and presentations

The project results and new knowledge (foreground) generated within the NASCEnT project were first considered from the point of view of intellectual right protection – patentability or necessity of keeping it as internal know-how for exclusive exploitation by the project consortium. Only then a part of results were published in scientific journals and presented at conferences and meetings. This work was effective and without any conflicts even in cases of foreground generated by collaboration of several partners.

At the time of the final report the list of publications contains about 40 papers in international journals and more than 50 presentations at conferences including 16 invited lectures. There are still some papers under preparation. In our opinion it is quite impressive results for such a medium size 3-years project.

The activities of NASCEnT project were also regularly presented at the main European PV meetings starting from the workshop Photovoltaic and Nanotechnology, European PV Projects Meeting at Aix Les Bains in 2010, European Photovoltaic Solar Energy Conferences and Exhibition and E-MRS meetings.

Transfer of knowledge and education

The project partners paid attention to the educative activities with the aim to prepare high-level young researchers for European PV industry and research institutions.

Several PhD and diploma students were involved in the R&D and demonstration work as part of their theses work. The preparation of an education-oriented book was already mentioned above.

D06.1 Technical exploitation roadmap

Promoting the use and dissemination of NASCEnT results was a key objective of the final stage of the project. All ideas and data were collected from partners in order to set-up the exploitation roadmap and write down the final *Plan for the use and dissemination of the foreground*, which is one of the most important documents prepared at the end of the NASCEnT project.

Potential impact

Strategic impact

The “multi-junction approach” is the most logical way to make use of the full spectrum of the sunlight. This is by no means a new idea. The realisation of this concept with **crystalline Si**-based materials however, is a **highly innovative approach**. Micromorph Si tandem solar cells have been investigated thoroughly, but no remedies for the degradation of the top amorphous Si solar cell could yet be identified. Si nanocrystal solar cells circumvent this problem and open the path for efficient tandem solar cells based on Si materials. A silicon quantum dot solar cell is the building block for devices that combine high-efficiency and low cost. The all-silicon tandem cell which has been realised within this project is compatible with standard silicon VLS production technologies and would boost both wafer-based and thin film technologies.

The project examined in detail open questions regarding nanocrystal doping, dielectric host matrices and their interfaces properties, mechanisms of charge carrier recombination and transport in Si nanocrystals and the host matrices.

These topics are of **high scientific interest** not only for **photovoltaics** but also for **novel photonic** and **charge storage** (flash memory) devices incorporating Si nanocrystals. Moreover the **computational routines** developed and the obtained theoretical results will reinforce the **leading position of Europe in this field** and will provide a genuine understanding of the dependence of the structural, opto-electronic and transport properties of semiconductor systems on their low- and nano-dimensionality. The development of device parts such as emitters, passivation layers, insulating layers, diffusion barriers and tunnel diodes for the material systems under investigation and the optimisation of process technologies implies a considerable profit for related technologies such as SiC power devices, charge storage and optoelectronics.

Another scientific impact may be mentioned: Since several members of the consortium are engaged in student education the findings of the project were immediately transferred to the “brains” of the next generation of young researchers in material science and photovoltaics

Silicon photovoltaics

Silicon is an abundant, evenly distributed material on the terrestrial surface, it is non-toxic and its application does not suffer from potential problems related to environmental pollution. However, despite the abundance of silicon in the earth crust, the cost of monocrystalline Si wafers has presently a severe impact on final costs of modules due to the high purification costs. Thin film approaches have the advantage that no purification and no block crystallisation step is needed. Furthermore they give the possibility of further cost reduction by large area deposition, low temperature processes and because they can sustain higher impurity levels.

Beside the material costs, cell production, module assembly and system installation are the main cost limiting factors. Larger production scales are a possibility to lower Levelised costs

of Electricity, but will saturate in the long term without innovation break through. Therefore, only higher cell efficiencies that are achieved with lower material and production costs can sustainably ensure a decrease of the *Levelised Costs Of Energy* (LCOE).

Supposing that the high efficiency anticipated for double junction solar cells will be obtained using the nc-Si/micro-Si, design, one cubic meter of silicon will be approximately the quantity needed for a 4 MW power plant. Even with more realistic efficiencies, using silicon as the base material for solar cells whose design implies a factor of approximately 50 times lower thickness with respect to standard industrial solar cells has a direct impact on reduction of the raw material consumption and on purification costs, and therefore on material-related final costs.

Thin-film solar cells furthermore allow the use of flexible substrates such as stainless steel but also plastics such as PEN or PET which is a very important advantage for applications like building integrated PV. Alternative medium- and high-efficiency potential competitors to thin film silicon like CdTe and CIGS are certainly extremely promising but require the use of materials that face severe drawbacks, such as copper, cadmium, indium, selenium, and tellurium. These material are not suited for the tens of GW annual production volumes of PV modules expected in the near future because they are costly, toxic, associated with severe manipulation concerns, much less abundant if not extremely rare, or available only in remote and/or politically instable countries.

The use of silicon quantum dot nanomaterials

Currently, most silicon-based tandem modules are based on either all-amorphous double or triple junction devices, or on micromorph solar cells (amorphous /microcrystalline double junction solar cells). Both designs suffer from the degradation of the a-Si:H (Staebler-Wronski effect) device under illumination, although in a reduced manner compared to single junction a-Si:H solar cells. The microscopic mechanism of degradation is the breaking of a distorted Si-Si bond and formation of two dangling bonds, and successive switching that brings them apart. Electrical degradation up to more than 16 % (relative value) typically occurs on such devices. Si-nanocrystal based solar cells are expected to overcome this problem. Due to the stability of the crystalline structure, no creation of dangling bonds occurs within the nanocrystal, with direct consequences for the stability of the photovoltaic device.

The idea of using Si-nanocrystals as **tuneable band gap material for photovoltaic** purposes has in fact triggered intense research activity on silicon nanocrystals in the last ten years. Besides a tuneable band gap, Si NC also show **increased oscillator strengths** due to a **more direct character of the band gap**. However, a photovoltaic device also came to work because the electrical properties, in addition to the optical properties, met the device requirements. In spite of this basic consideration, only **limited information on the electrical behaviour** of Si NC composite materials was available at the beginning of the project and the identification of “ideal” or required electrical properties as a solar cell material is one major outcome of this project.

NASCEnt answered many of these questions. The understanding of electrical transport and recombination mechanisms in the newly developed nanomaterials enabled us to design novel solar cell structures that will help to overcome the efficiency limits of conventional solar cell concepts. The needed material specification have been defined, and a clear picture of the electrical behaviour of Si QD's is now available. The direct comparison of three different host materials for Si NC led to a much more detailed understanding of the solid state crystallisation mechanisms of Si in different host matrices and the electronic properties of the compound material.

The attained ability of controlling such properties already has dramatic impact on the applicability of Si QD's to photovoltaic, and, more generally, to electrical devices.

Impact at device level

For a tandem photovoltaic device composed of two semiconductors with 1.1 eV and 1.7 eV for the band gap of the bottom and top device respectively, a maximum theoretical efficiency of 39 % to 45 %, depending on the theoretical model, is estimated. Actual silicon-based tandem devices with an amorphous silicon top cell show efficiencies in the range of 10 %-14 %. This value indicates a large potential for improvement, but the discrepancy also evidences the need for an accurate device design and tuning of the materials electrical properties. The major limitations of actual silicon based tandem devices arise from a number of reasons: high defect density and limited mobility of the amorphous device; limited thickness of the top device to achieve current matching, and others. A QD-Si material with low defect density, able to ensure a low reverse saturation current and therefore a higher current density and an open circuit voltage V_{oc} that is closer to the theoretical limit, will result in higher efficiency of the photovoltaic device.

An additional exploitation of the confined Si nanostructure concept studied by the **NASCEnt** consortium is in the area of crystalline Si PV. Silicon wafer-based tandem devices are expected to show higher efficiencies with respect to both thin-film tandem and single junction wafer-based devices. In the first case, this is due to the larger thickness of the bottom cell leading to higher current densities, and to the better electronic properties. In the second case the advantage is associated with the significantly improved blue response and the higher voltage of the top device. In both cases, a decrease of the contribution of the material cost to the final cost of the installed power is foreseen.

Theoretical impact

The theoretical investigations already show the full potential of the computational approaches toward a better understanding of the quantum confinement effects, energy transfer, radiative decay, non radiative decay and trapping, determining the key parameters that should be met for the ultimate application of silicon nanocluster ensembles for solar light harvesting. Beside the treatment of the pure nanocrystal system, the role of dopants and the role of the surrounding matrix and the interface between the nanocrystals and the matrix have been investigated. These topics targeted the main yet unsolved questions concerning Si nanocrystals. Theoretical investigations of the role of dopants are highly necessary to advance also experimentally towards controlled doping of nanostructures.

Understanding the influence of the surrounding matrix and the interface enables now an assessment of potential dielectrics and the role of defects in those. The computational routines developed and the obtained theoretical results reinforced the leading position of Europe in this field and will provide a genuine advance in the comprehension of the dependence of the structural, opto-electronic and transport properties of semiconductor systems on their low- and nano-dimensionality.

Scientific and industrial progress in related disciplines

The project has been investigating in detail open questions regarding nanocrystal doping, dielectric host matrices and their interfaces properties, mechanisms of charge carrier recombination and transport in Si nanocrystals and the host matrices. Besides photovoltaics, these topics are of high scientific interest for novel photonic and charge storage (flash memory) devices incorporating Si nanocrystals.

In addition, the development of device parts such as emitters, passivation layers, insulating layers and tunnel diodes for the material systems under investigation and the optimisation of process technologies implies a considerable profit for related technologies such as SiC power, charge storage and optoelectronic devices.

Economic impact

There is no doubt that the success of this project will have an economic impact for the European PV Industry. The breakthrough for crystalline silicon and a-Si based PV can lead to much reduced costs and real mass production. Given that industry is ready to realise our concept in an industrial scale it could boost the PV industry that produces these systems.

For more than thirty years, the most important parameter governing the growth of installed PV, i.e. the average delivered power per Euro in commercial PV modules, has improved continuously with a classical learning curve trend, corresponding to approximately 20 % cost decrease per doubling of the installed PV power. PV industry has been facing for almost a decade the impressive growth of about 40 %. Such growth has been dominated by silicon wafer based PV in the form of mono- and multi-crystalline silicon, covering about 90% of the market. However, the total contribution of PV to energy production is still marginal (around 0.1 %). The reason for this is the high cost of PV energy compared to other sources, also including other renewables such as wind or hydroelectric. In fact the huge PV industry growth has been so far heavily sustained by state incentives, put in place first in Japan and then in Germany and Spain, later followed by other nations such as Italy and France. In the last few years this trend has been strongly broken due to the occurrence of a silicon shortage. In fact, the large growth of the PV market together with the needs of the microelectronics industry resulted in a total amount of requested silicon feedstock above the worldwide production capacity. This implied an increase of the price of the silicon feedstock which has resulted in the cost of the silicon modules remaining high.

On the other hand there is a growing consensus that the sun, and in particular PV, is likely the best source at the global level for sustainable energy production, given its far better potential than other renewables in terms of the total availability of energy. However, to meet

such goals PV needs to solve major cost issues at the module as well as at the system level.

NASCENT addressed the energy cost challenge from the side of the module cost, by proposing an innovative concept for the realisation of PV devices suitable for industrial up scaling, and this is, we believe, among the major merits of the project.

In the PV race, the industry is in fact extremely dynamic, playing a major role in the innovation. This is indeed demonstrated by the recent evolutions in the field, where the Japanese players have partially lost their top positions in favour of new companies. But the race is far from over, with new strong, fast and dynamic players growing out of the U.S., China, and Taiwan. In some cases rapid innovations, also quite radical, are the origin of their rise.

This vitality is clearly the base for the impressive growth perspectives expected by the PV industry in future: although the total required energy at the global level is expected to grow by about 0.4 TW/year, the energy fraction produced by PV should grow enormously, by reaching the 1 % milestone in the next few years and going up to the 2 % level in 2020, with an overall market of about 140 Billion €. Nowadays the European presence in the module production race is good, with one big player (Q-Cells) in the top-ten ranking, but this is a rapidly moving field, so the situation may change fast. For example, just in 2001 in the top ten ranking the European presence was much stronger. This circumstance is a clear indicator for the need of pushing the European research in the PV field to the maximum extent, in order to maximise the share of European Companies for this surely very promising area of business.

The existence in Europe of a technology able to circumvent actual limitations due to high costs could have a positive impact on the acceptance of photovoltaics by the public and by politics, with the potential of creating a break-through for silicon based PV to real mass production, and eventually bringing Europe to the head of PV market share and to an important position in the overall energy production context, with outcomes on several areas, here included world social stability.

The **technology** applied within **NASCENT** makes use of high vacuum deposition machines such as Plasma Enhanced Chemical Vapor Deposition (PECVD) and high temperatures furnaces or Rapid Thermal Annealing (RTA) equipments and may not be regarded as a low-cost technology. However, both equipments are already present in a standard wafer based solar cell production line: a PECVD apparatus is required for the SiN_x anti-reflection coating and passivation layer deposition, while furnaces are needed in the dopant diffusion process for the formation of the emitter and the back surface field (BSF). The furnace annealing of QD's as applied within NASCENT even reduces the energy consumption, compared with the dopant diffusion time. In contrast, the PECVD deposition of the Si rich superlattice will require longer deposition time compared to the SiN_x passivating layer. This may be a concern, however, the use of VHF-based PECVD in comparison to standard RF deposition, goes in the direction of reducing the deposition time. It is just the case to remind that the technology of the widely diffused amorphous silicon technology makes actually use

of RF PECVD deposition, and that the same technique, yet based on VHF, exactly for the same reason, is in fact used in the fabrication of the microcrystalline layer in the technology of the amorphous/crystalline (“micromorphe”) silicon tandem solar cells.

The achievement of grid parity will have the immediate consequence of making PV electricity convenient with respect to conventional sources. In such a scenario, the great expectations of the PV industry in the near and far future (see Table 3) may be met or even exceeded. Si thin-film technologies could play a major role in this scenario if boosted by the confined Si nanostructures tandem solar cell concept.

Table 3: Solar Generation scenario results for global PV market up to 2030¹.

	Current situation	Scenarios		
	2007	2010	2020	2030
Advanced Scenario				
Annual Installations in GW	2.4	6.9	56	281
Accumulated Capacity GW	9.2	25.4	278	1,864
Electricity Production in TWh	10	29	362	2,646
PV Contribution to electricity consumption - reference scenario (IEA)	0.07%	0.16%	2.05%	8.90%
PV Contribution to electricity consumption - alternative scenario	0.07%	0.20%	2.18%	13.79%
Grid connected people / households / people living on PV in Million	5.5	18	198	1,280
Off grid connected people in Million	14	32	757	3,216
Employment in thousand people	119	333	2,343	9,967
Market value in Billion €	13	30	139	454
Annual CO ₂ savings in Mt	6	17	217	1,588
Cumulative carbon savings in Mt	27	65	976	8,953

The presence of very promising results on QD-Si devices achieved by **NASCEnT** will hopefully attract money and activity, with the potential of creating start-ups, with people working on the topic and economic benefits. There will be the possibility of better focussing of the money allocated to PV, and more efficient utilisation of resources, with all outcomes expected from a convenient renewable source only delayed to a less near future.

In summary, we believe that the **NASCEnT** project, putting together unique know-how from different EU member states, will have direct and positive impact on the European PV industry and its status in material science. It will also contribute to the very ambitious goal of the EU commission concerning the CO₂ reduction in general.